Nuclear Magnetic Resonance

Author: Sean Ballinger
Partners: Adam Mathieu, Norman Watson

March 28, 2014

Abstract

The gyromagnetic ratio and magnetic moment of several atoms were calculated using nuclear magnetic resonance. For the proton, samples of diluted $CuSO_4$ were used, and for the deuteron, D_2O. The magnetic moment of each particle was calculated from its gyromagnetic ratio, and the fundamental quantity of the ratio of the magnetic moment of the deuteron to that of the proton was calculated. The gyromagnetic ratio of the ^{19}F fluorine nucleus was also determined using a sample of Teflon, and we observed the saturation of relaxation times for samples of varying concentrations of cupric sulfate. The accepted values of measured quantities fell within in the error range of experimental results, which was determined using the gradient of the magnetic field strength and the accuracy of the Hall effect gaussmeter.

1 Introduction

The spinning charge of an atom with an odd number of protons or neutrons gives rise to a magnetic moment. Electromagnetic radiation is absorbed and re-emitted at a frequency specific to the atom and directly proportional to the magnetic field strength. This frequency is called the resonance frequency, and these properties make possible the use of nuclear magnetic resonance (NMR) for spectroscopy and medical imaging, in which applying a non-uniform field and noting the resonance frequency of an atom can betray its location [1].

The principle of this experiment was to drive the magnetic moment of different atoms between adjacent energy levels using a constant magnetic field and an oscillating, perpendicular one, along with RF waves in the MHz regime, to observe each atom's resonance frequency at different levels of magnetic field strength [2]. This makes it possible to precisely determine the constant behind their linear relationship, called the gyromagnetic ratio, and subsequently the magnetic moment, for each atom.

2 Preliminary Measurements

2.1 Magnetic Field

A Hall effect gaussmeter with .25% accuracy, which uses the fact that charge carriers flowing through a conductor are displaced in the presence of a magnetic field, was used to determine the maximum strength of the magnetic field produced by the electromagnet. The gaussmeter was calibrated at the center of a conducting cylinder.

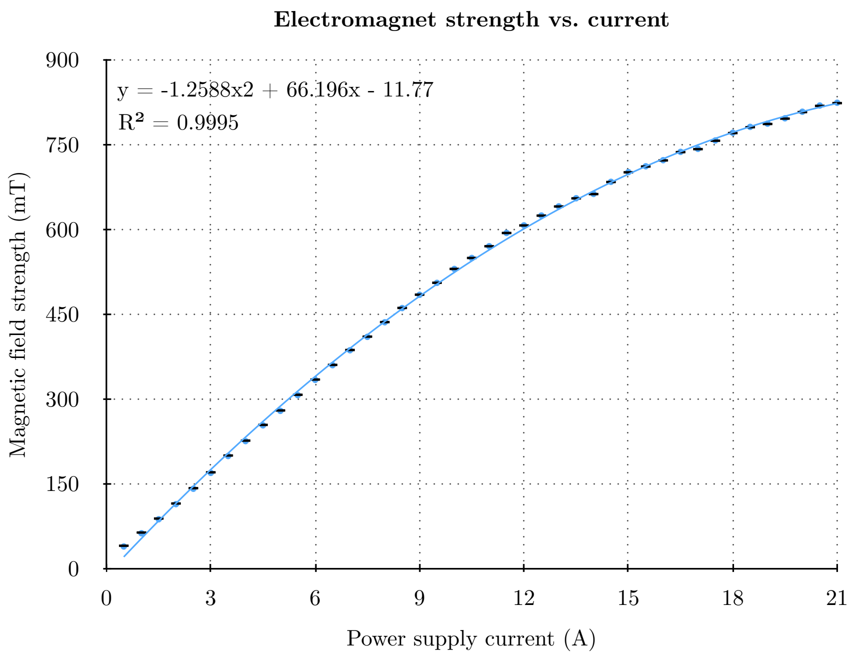

FIGURE I: Plot of magnetic field as a function of the current from the power supply. Error bars indicate .25% uncertainty in gaussmeter measurements. Data fit using a quadratic regression.

Apparent on this graph are two approximately linear segments of differing slope. The change occurs around 12 A of current supplied to the electromagnet, and shows the point at which the magnetic domains in the material, initially of random orientation, have all lined up to add to the external magnetic field, so the overall strength grows less rapidly [3]. We say that the iron core of the electromagnet has become saturated after 12 A.

2.2 More Accurately Determining the Magnetic Field

Resonance at a range of different electromagnet current values for a sample of cupric sulfate ($CUSO_4$) was used to more accurately determine the magnetic field at the location of the sample for each level of current.

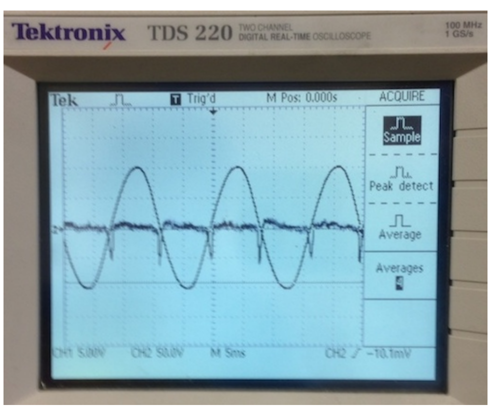

FIGURE II: Voltage peaks observed at resonance conditions for $CuSO_4$ sample.

At each level of current, the oscillator frequency was tuned until resonance was observed. As can be seen in figure II, there is some small error associated with how we define the resonance frequency, and in some cases it is impossible to line up all the signal peaks with the nodes of the sinusoid. This error is specific to each sample and magnetic field strength being used, as adjustments in the RF frequency can have differing effects on the positioning of the peaks. The value indicated on the frequency meter was translated to a magnetic field measurement using the accepted value of the proton gyromagnetic ratio of 42.577 MHz/T [4]. For example, at 18 A, where we observe resonance at 32.85 MHz:

$$\frac{32.85 \text{ MHz}}{42.577 \text{ MHz/T}} = .7715 \text{ T} \tag{1}$$

This was performed for a series of points in the range of 18–21 Ampères.

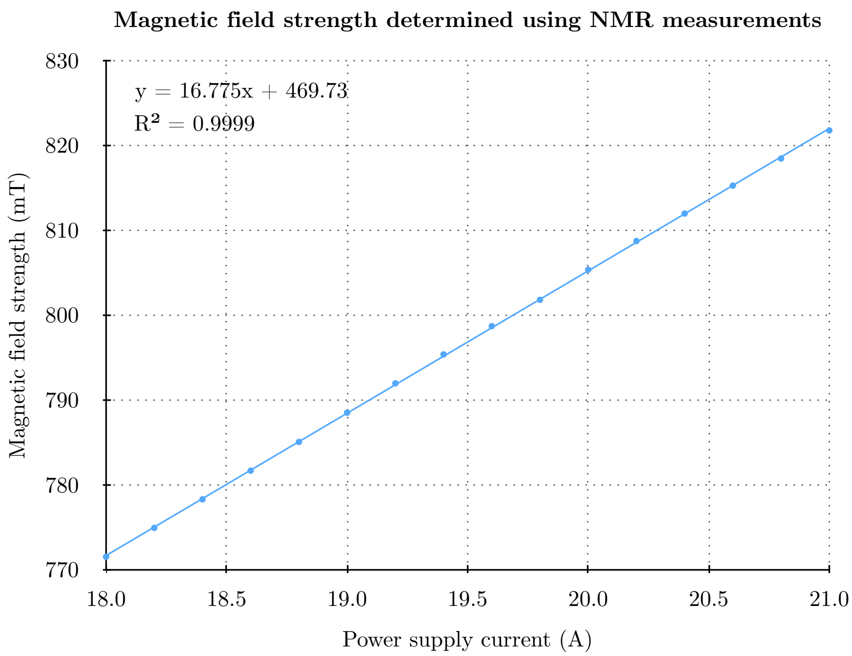

FIGURE III: Plot of magnetic field as a function of current from the power supply. Data fit using a linear regression.

The formula obtained in figure III allows us to precisely determine the magnetic field in the range of electromagnet operation where further measurements were conducted.

2.3 Error in Magnetic Field Measurements

Because the magnetic field strength measurements using NMR are specific to the placement of the $CuSO_4$ sample used on that day, we must determine error bounds on magnetic field strength for later samples that draw on this data. We do so by evaluating two gradients of the magnetic field strength in the electromagnet, using data from the hall probe.

Figure IV: Polar grid used to record hall probe position.

A polar grid was set up to measure the magnetic field strength at various positions in the electromagnet for operation at 18 A.

Angle	$\mathbf{R_1}$ **(2cm) (mT)**	$\mathbf{R_2}$ **(4cm) (mT)**
0	773.8	760.5
$\pi/4$	775.3	767.8
$\pi/2$	776.5	764.0
$3\pi/4$	776.1	752.2
π	776.0	746.3
$5\pi/4$	775.6	740.1
$3\pi/2$	773.5	735.0
$7\pi/4$	773.9	758.2

Table 1: Magnetic field strength at various positions in the electromagnet.

The values in table 1 (and the maximum at the center of the electromagnet, 776.6 mT) were used to determine the change in magnetic field in two different directions near the position of the sample.

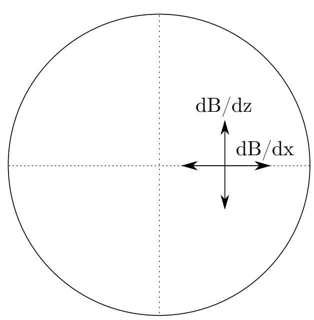

Figure V: Calculating variation in magnetic field strength near position of sample.

By evaluating the change in magnetic field relative to the radius of the probe (1.9 cm) in the x and z directions, we obtain a maximum error for the magnetic field in the testing region:

$$dB_x = \frac{|B(R_2, 0) - B(0,0)|}{2} dx = 15.30 \text{ mT} \quad (2)$$

$$dB_z = \frac{|B(R_1, \pi/4) - B(R_1, 7\pi/4)|}{\sqrt{2}} dz = 1.881 \text{ mT} \quad (3)$$

We add (2) and (3) in quadrature to get the total error in magnetic field measurement:

$$dB_{\text{tot}} = \sqrt{(dB_x)^2 + (dB_z)^2} = 15.41 \text{ mT} \quad (4)$$

To obtain an error percentage, we compare the result of (4) to the magnetic field determined using NMR of $CuSO_4$ in section 2.2:

$$\frac{15.41}{771.54} = 2.00\% \quad (5)$$

3 Gyromagnetic Ratio of the Proton

A sample of $CuSO_4$ was used to determine the gyromagnetic ratio of the proton. The magnetic field was calculated using the quadratic fit obtained from figure I:

$$B = \frac{-1.2588I^2 + 66.196I - 11.77}{1000\ \text{mT/T}} \tag{6}$$

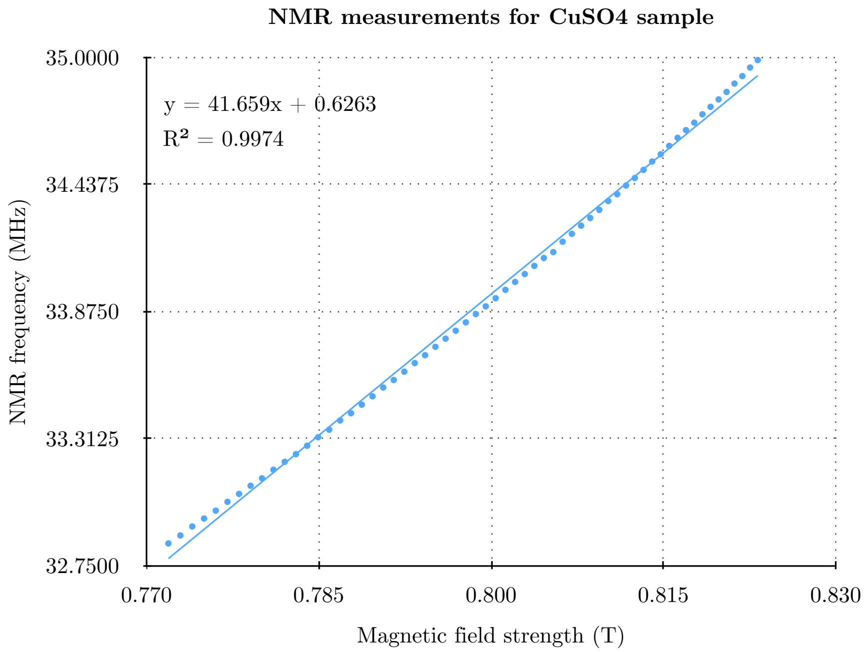

FIGURE VI: Plot of NMR frequency as a function of magnetic field strength for a $CuSO_4$ sample. Data fit using a linear regression, its slope corresponding to the gyromagnetic ratio of the proton.

The gyromagnetic ratio of the proton $\gamma_p/2\pi$ is obtained from the slope of the linear regression, which in figure VI we see to be 41.659 MHz/T. Using our error calculated in (5) in addition to the .25% error of the Hall probe, we obtain

$$\gamma_p/2\pi = 41.659 \pm .940\ \text{MHz/T}. \tag{7}$$

The accepted value of 42.577 MHz/T [4] falls within this range.

We can also calculate the proton magnetic moment μ_p as follows:

$$\mu_p = \gamma_p \cdot \hbar/2 = 41.659 \cdot 10^6 \cdot 1.056 \cdot 10^{-34} \cdot \pi = (1.380 \pm .0312) \cdot 10^{-26}\ \text{J/T}. \tag{8}$$

The accepted value of $1.410 \cdot 10^{-26}$ J/T [5] falls within range of this quantity's error.

4 Gyromagnetic Ratios of Other Nuclei

4.1 Fluorine

A sample of Teflon, a perfluorinated hydrocarbon, was used to determine the gyromagnetic ratio for the nucleus of fluorine, ^{19}F.

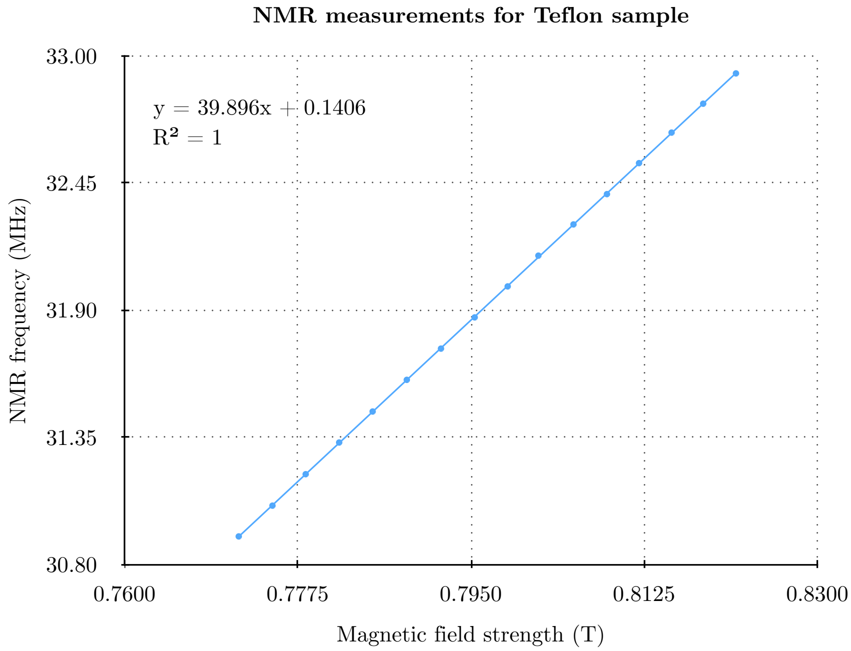

FIGURE VII: Plot of NMR frequency as a function of magnetic field strength for a Teflon sample. Data fit using a linear regression, its slope corresponding to the gyromagnetic ratio of the fluorine nucleus.

Again, the gyromagnetic ratio of the fluorine nucleus $\gamma_F/2\pi$ is obtained from the slope of the linear regression, which in figure VII we see to be 39.896 MHz/T. Using the error calculated in (5) (no error from the Hall probe in this case because NMR was used to determine the magnetic field), we obtain

$$\gamma_F/2\pi = 39.896 \pm .8011 \text{ MHz/T}. \tag{9}$$

The accepted value of 40.053 MHz/T [6] falls within this range.

4.2 The Deuteron

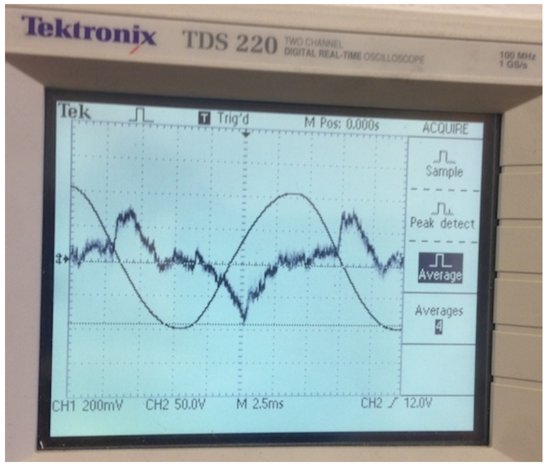

FIGURE VIII: Resonance voltage peaks for the deuteron against significant background noise.

The deuteron was a challenge to measure, because NMR could only be observed at a much lower frequencies of around 5 MHz, and the signal was barely visible against significant background noise, as shown in figure VIII.

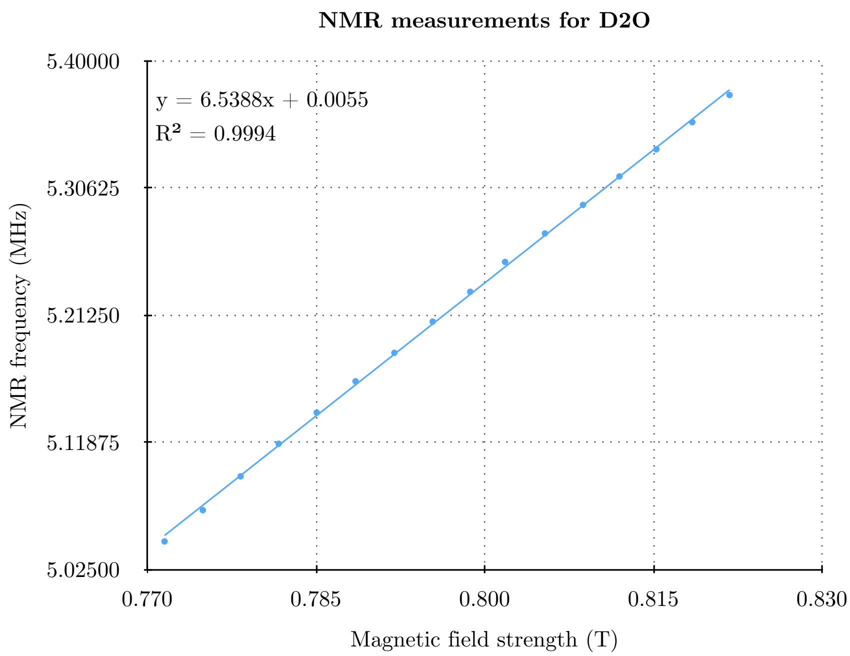

FIGURE IX: Plot of NMR frequency as a function of magnetic field strength for a D_2O sample. Data fit using a linear regression, its slope corresponding to the gyromagnetic ratio of the deuteron.

The gyromagnetic ratio of the deuteron $\gamma_d/2\pi$ is obtained from the slope of the linear regression, which in figure IX we see to be 6.5388 MHz/T. Using the error calculated in (5), we obtain

$$\gamma_d/2\pi = 6.5388 \pm .1308 \text{ MHz/T}. \tag{10}$$

The accepted value of 6.536 MHz/T [6] falls within this range.

We can also calculate the deuteron magnetic moment μ_d as follows:

$$\mu_d = 2\gamma_d \cdot \hbar/2 = 4\pi \cdot 6.5388 \cdot 10^6 \cdot 1.056 \cdot 10^{-34}/2 = (4.333 \pm .08665) \cdot 10^{-27} \text{ J/T}. \quad (11)$$

This is within range of the accepted value of $.433 \cdot 10^{-26}$ J/T [7].

4.2.1 μ_d/μ_p

We use our calculated values of γ_p and γ_d to determine the fundamental quantity μ_d/μ_p:

$$\mu_d/\mu_p = 4.333/13.80 = .3140 \quad (12)$$

The accepted value is .307 [8]. The discrepancy is likely due to the differences in positioning for the measurements of γ_p and γ_d, which were determined in separate sessions.

5 Relaxation Saturation Effect

With the electromagnet operating at a constant 20 A, samples of varying concentrations of cupric sulfate were observed for NMR, and the amplitude of the signal peaks in each case was recorded.

FIGURE X: Variously diluted solutions of cupric sulfate.

The rightmost beaker in figure X shows the maximum saturation of $CuSO_4$ in solution, in which any additional particles would not dissolve.

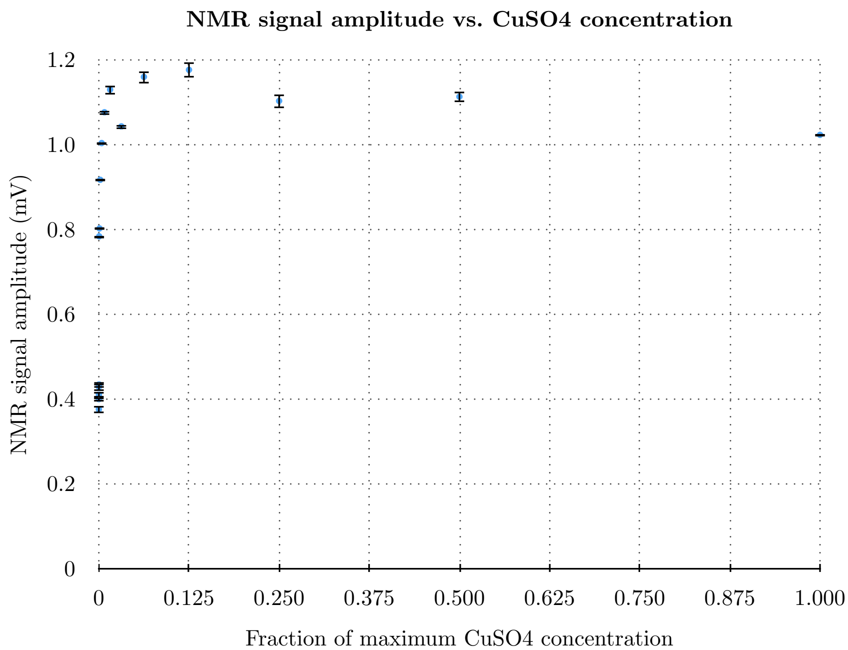

FIGURE XI: NMR signal amplitude observed for variously diluted solutions of cupric sulfate.

Figure XI shows the NMR signal amplitude as a function of the relative concentration of $CuSO_4$, which shows the mean of three peaks' amplitudes and error bars indicating the standard deviation of the mean.

We observe that at the start of the curve, signal strength grows according to

$$S \propto M_{eq}(\Gamma_0 + c\Gamma_1)\tau, \tag{13}$$

where M_{eq} is the magnetization and Γ_0 and Γ_1 correspond to the relaxation rates of water and copper, respectively. We see that as the concentration c of copper increases in the $CuSO_4$ solution, the higher relaxation rate of copper Γ_1, due to its larger magnetic moment, quickly becomes more significant. The curve is then better described by the relation

$$S \propto (1 - x)M_{eq} \tag{14}$$

where x is the flipping fraction [2].

6 Conclusion

The gyromagnetic ratios of the proton, deuteron, and fluorine nucleus were measured. The magnetic moment of the proton and neutron were calculated, and the fundamental quantity of their ratio was obtained. The relaxation saturation effect was observed for by varying the concentration of cupric sulfate in solution. Further analysis could involve the calculation of the magnetic moment of the neutron from that of the proton and deuteron using the Landé g-factor [2].

This experiment made it possible to explore the basic principles behind NMR's use in imaging and spectroscopy. It is notable that the high gyromagnetic ratio of the proton (which we calculated to be 41.659 MHz/T, much larger than 6.5388 MHz/T for the deuteron but not much greater than the fluorine nucleus' 39.896 MHz/T) makes it useful in medical imaging to obtain a strong signal [9].

References

[1] Nuclear magnetic resonance. (2014, March 24). *Wikipedia, The Free Encyclopedia.* Retrieved March 28, 2014, from http://en.wikipedia.org/wiki/Nuclear_magnetic_resonance

[2] Nachumi, B. (2013). *NMR 1: LF NMR.* 1–14.

[3] Electromagnet. (2014, March 24). *Wikipedia, The Free Encyclopedia.* Retrieved March 28, 2014, from http://en.wikipedia.org/wiki/Electromagnet

[4] CODATA value: proton gyromagnetic ratio. *NIST.* Retrieved March 28, 2014, from http://physics.nist.gov/cgi-bin/cuu/Value?gammapbar|search_for=proton+gyromagnetic+ratio+over+2+pi

[5] CODATA value: proton magnetic moment. *NIST.* Retrieved March 28, 2014, from http://physics.nist.gov/cgi-bin/cuu/Value?mup|search_for=proton+magnetic+moment

[6] Gyromagnetic ratio. (2014, March 18). *Wikipedia, The Free Encyclopedia.* Retrieved March 28, 2014, from http://en.wikipedia.org/wiki/Gyromagnetic_ratio

[7] CODATA value: deuteron magnetic moment. *NIST.* Retrieved March 28, 2014, from http://physics.nist.gov/cgi-bin/cuu/Value?mud|search_for=deuteron+magnetic+moment+

[8] CODATA value: deuteron-proton magnetic moment ratio. *NIST.* Retrieved March 28, 2014, from http://physics.nist.gov/cgi-bin/cuu/Value?mudsmup|search_for=deuteron-proton+magnetic+moment+ratio

[9] Magnetic Resonance Imaging. (2008). *Scholarpedia: The Peer-reviewed Open-access Encyclopedia.* Retrieved March 28, 2014, from http://www.scholarpedia.org/article/MRI